Title

Sex and age modify biochemical and skeletal manifestations of chronic hyperparathyroidism by altering target organ responses to Ca2+ and parathyroid hormone in mice.

Journal

Journal of bone and mineral research : the official journal of the American Society for Bone and Mineral Research, 28(5)

ISSN

0884-0431

Authors

Cheng, Zhiqiang
Liang, Nathan
Chen, Tsui-Hua
et al.

Publication Date

2013-05-01

DOI

10.1002/jbmr.1846

Peer reviewed

Published in final edited form as:
J Bone Miner Res. 2013 May ; 28(5): 1087–1100. doi:10.1002/jbmr.1846.

Sex and Age Modify Biochemical and Skeletal Manifestations of Chronic Hyperparathyroidism by Altering Target Organ Responses to Ca^{2+} and PTH in Mice

Zhiqiang Cheng, **Nathan Liang**, **Tsui-Hua Chen**, **Alfred Li**, **Christian Santa Maria**, **Michael You**, **Hanson Ho**, **Fuqing Song**, **Daniel Bikle**, **Chialing Tu**, **Dolores Shoback**, and **Wenhan Chang***
Endocrine Research Unit, Department of Veterans Affairs Medical Center, Department of Medicine, University of California, San Francisco, CA 94121, USA

Abstract

We studied mice with or without heterozygous deletion of the *Casr* in the parathyroid gland (PTG) [^{PTG}CaSR(+/−)] to delineate effects of age and sex on manifestations of hyperparathyroidism (HPT). In control mice, aging induced a left-shift in the Ca^{2+}/parathyroid hormone (PTH) set-point accompanied by increased PTG CaSR expression along with lowered serum Ca^{2+} and mildly increased PTH levels, suggesting adaptive responses of PTGs to aging-induced changes in mineral homeostasis. The aging effects on Ca^{2+}/PTH set-point and CaSR expression were significantly blunted in ^{PTG}CaSR(+/−) mice who showed instead progressively elevated PTH levels with age, especially in 12-month-old females. These 12-month-old knockout mice demonstrated resistance to their high PTH levels in that serum 1,25-dihydroxyvitamin D (1,25-D) levels and RNA expression of renal Cyp27b1 and expression of genes involved in Ca^{2+} transport in kidney and intestine were unresponsive to the rising PTH levels. Such changes may promote negative Ca^{2+} balance, which further exacerbate the HPT. Skeletal responses to HPT were age-, sex-, and site-dependent. In control mice of either sex, trabecular bone in the distal femur decreased while cortical bone in the tibiofibular junction increased with age. In male ^{PTG}CaSR(+/−) mice, anabolic actions of the elevated PTH levels seemed to protect against trabecular bone loss at ≥3 months of age at the expense of cortical bone loss. In contrast, HPT produced catabolic effects on trabecular bone and anabolic effects on cortical bone in 3-month-old females; but these effects reversed by 12 months, preserving trabecular bone in aging mice. We demonstrate that the CaSR plays a central role in the adaptive responses of parathyroid function to age-induced changes in mineral metabolism and in target organ responses to calciotropic hormones. Restraining the ability of the PTG to upregulate CaSRs by heterozygous gene deletion contributes to biochemical and skeletal manifestations of HPT, especially in aging females.

Introduction

Skeletal development and mineral homeostasis are tightly controlled by the secretion and actions of PTH and 1,25-D in target tissues. Parathyroid cells -- first responders in this homeostatic paradigm -- function as “calciostats” to detect subtle changes in the serum [Ca^{2+}] and respond with altered PTH secretion (1-3). Lowering the extracellular Ca^{2+} concentration ([Ca^{2+}]$_e$) rapidly induces PTH secretion. PTH promotes Ca^{2+} reabsorption in

*Corresponding author: Wenhan Chang, PhD, Endocrine Research Unit, 111N, San Francisco Department of Veterans Affairs Medical Center, 4150 Clement Street, San Francisco, CA 94121, USA. Telephone: 415-750-2089. Fax: 415-750-6929. Wenhan.Chang@ucsf.edu.

Disclosure: The authors state that they have no conflicts of interest

the kidney by increasing the expression and activity of transient receptor potential cation channel subfamily V member 5 (TRPV5) (4). PTH enhances renal Cyp27b1 expression and activity to produce 1,25-D (5-8) that increases intestinal Ca^{2+} absorption by promoting the expression and/or activity of TRPV6 channels, calbindin (CalB), and plasma membrane Ca^{2+} ATPase (PMCA) in the intestine (9-12). PTH also increases bone remodeling to mobilize Ca^{2+} from bone matrix (13,14). Together these actions restore serum [Ca^{2+}] to normal. A rise in the $[Ca^{2+}]_e$ or in the 1,25-D level feeds back to suppress PTH secretion by activating the extracellular Ca^{2+}-sensing receptor (CaSR) and the vitamin D receptor (VDR), respectively, preventing an overshoot in PTH and the undesired consequence of hypercalcemia. Deviations from this regulation lead to abnormal mineral and skeletal homeostasis.

Primary hyperparathyroidism (HPT) is a common endocrinopathy due to either adenoma(s) or multi-gland hyperplasia (15-18). The etiology of the disease is unclear, except for the minority of cases clearly linked to genetic defects (19-22). The disease is common in older adults, especially postmenopausal females (23). Possibly their susceptibility increases as a consequence of estrogen deficiency or aging. Alternatively, responsiveness to PTH or 1,25-D in target organs (gut, kidney, bone) may contribute, or a combination of these mechanisms may be responsible.

Studies have shown reduced CaSR expression in tumors from patients with primary or secondary HPT (24,25). This suggests that reduced extracellular Ca^{2+}-sensing by PTGs may increase the propensity to develop HPT and/or for it to progress to the point of clinical detection. The effects of aging and sex on CaSR expression in PTGs from normal humans have not been studied systemically. In male rats, CaSR RNA and protein expression in PTGs actually increase with age (26). Thus, reduced CaSR expression in glands from patients with HPT may be a result of the genetic or environmental factors that cause the disease and not the aging process itself.

With aging, humans develop negative Ca^{2+} balance, likely due to declining renal and intestinal function and other factors, and serum PTH levels modestly increase (27-29). Clearly, the aging process produces imbalances between the capacity of the target organs (intestine, kidney, and bone) to close all the feedback loops in response to PTH and 1,25-D. These imbalances may alter parathyroid cell proliferation and activity, which may underlie the increased incidence of HPT with age. We hypothesize that increased CaSR expression in PTGs is a physiological adaptation to the progressive Ca^{2+} deficit (due to target-organ resistance to PTH and 1,25-D) in aging; that CaSR expression increases to control the increasing PTH pool; and that conditions constraining this putative adaptive response of the PTGs (i.e., an inability to upregulate CaSR expression) facilitate the development of HPT. The increased propensity to develop HPT in elderly females also suggests that factors related to their sex could impact disease development by altering the responses of PTGs and other target organs to the calciotropic hormones that subsequently affect serum minerals, hormones and disease presentation.

The interactions of age and sex with the development of human HPT are important clinical issues that cannot be addressed directly because of practical constraints. Existing mouse models also have significant limitations. Transgenic mice overexpressing PRAD1 in the PTG develop HPT only at advanced age (30), precluding the study of the aging process on HPT. Prior studies of a generalized *Casr* gene knockout mouse model showed severe neonatal and generally lethal hypercalcemic HPT with homozygous *Casr* deletion and mild hypercalcemia in the heterozygous state [*Casr(+/−)*] (31). Impaired CaSR functions in other tissues due to CaSR haploinsufficiency, for example in intestine, kidney, bone, and cartilage

(31), complicate the interpretation of the effects of high serum Ca^{2+} and PTH levels in this model.

We studied mice with heterozygous deletion of the *Casr* gene targeted to parathyroid cells – a strategy that mimics the reduced CaSR number seen in primary HPT -- without disturbing Ca^{2+}-sensing in other tissues. These mice developed high serum PTH and Ca^{2+} levels by 2 weeks of age and demonstrated age- and sex-specific biochemical and skeletal responses to their increased serum PTH and Ca^{2+} levels. Our studies not only revealed novel adaptive responses in the PTGs, intestinal epithelium, kidney, and bone to changes in serum PTH and Ca^{2+} levels in an age- and sex-dependent manner, but also confirmed a central role for the parathyroid CaSR in development of HPT.

Materials and Methods

Generation of PTG-specific *Casr* knockout mice

Homozygous and heterozygous PTG-specific *Casr* knockout mice [^{PTG}CaSR(−/−) and ^{PTG}CaSR(+/−), respectively] were generated by breeding floxed CaSR mice (32), which carry lox-P sequences flanking exon 7 of the *Casr* gene (CaSR$^{flox/flox}$) with mice expressing Cre recombinase under the control of the PTH gene promoter [^{PTH}Cre(+/−)] (39). The mice were genotyped and kept in a climate-controlled room (22°C; 45-54% relative humidity) with a 12-hour light/12-hour dark cycle as previously described (32). Water and standard chow, containing 1.3% calcium and 1.03% phosphate, were given *ad libitum*. All experiments were approved by the Institutional Animal Care and Use Committee at the San Francisco Department of Veterans Affairs Medical Center.

Serum chemistries—Blood was drawn by cardiac puncture after euthanasia by isoflurane inhalation followed by tissue harvests. Serum samples were prepared by a microtainer serum separator tube (#365956, BD, Franklin Lakes, NJ), and analyzed for total serum Ca^{2+} (sCa) and inorganic phosphate (sPi), albumin, and creatinine by an automated ACE Alera® Clinical Chemistry bioanalyzer (Alfa Wassermann, Inc., West Caldwell, NJ). Serum intact PTH (sPTH) and 1,25-D levels (s1,25-D) were assessed using commercial ELISA kits made by Immutopics (San Clemente, CA) and Immunodiagnostic Systems Inc (Scottsdale, AZ), respectively.

Quantitative real-time polymerase chain reaction (qPCR) assays—RNA samples isolated from the kidneys and intestinal epithelium scraped off the first 2 cm of duodena from 3-12 month-old mice were reverse-transcribed into cDNA and subjected to qPCR (32-34) for expression of genes specified using Taqman-based sets of primers and probes.

Microcomputed tomography (μCT)—To assess mineral content and structure, we performed μCT scans at two sites: distal femur for trabecular (Tb) bone and tibio-fibular junction (TFJ) for cortical (Ct) bone as described (35,36). Briefly, femurs and tibiae were fixed in 10% phosphate-buffered formaldehyde (PBF) for 24 hrs, stored in 70% ethanol, and scanned by a SCANCO vivaCT 40 scanner (SCANCO Medical AG, Basserdorf, Switzerland) with 10.5 μm voxel size and 55 kV X-ray energy. For Tb bone in the distal femoral metaphysis, 100 serial cross-sectional scans (1.05 mm) of the secondary spongiosa were obtained from the end of the growth plate extending proximally. For Ct bone, 100 serial cross-sections (1.05 mm) of the tibia were obtained from the TFJ extending proximally. A threshold of 420 mg hydroxyapatite (HA)/mm^3 was applied to segment total mineralized bone matrix from soft tissue. Additional thresholds (420-1400 and >1400 mg HA/mm^3) were applied in some analyses to quantify low-density bone (LDB) and high-density bone (HDB) fractions in Ct bone, respectively. Linear attenuation was calibrated

using a μCT HA phantom. μCT image analysis and 3D reconstructions were done using the manufacturer's software to obtain the following structural parameters: Tb tissue volume (Tb.TV), Tb bone volume (Tb.BV), Tb.BV/TV ratio, Tb number (Tb.N), Tb connectivity density (Tb.CD), Tb thickness (Tb.Th), Tb spacing (Tb.Sp), Ct tissue volume (Ct.TV), and Ct thickness (Ct.Th).

Von Kossa (VK), Goldner, and tartrate-resistant acid phosphatase (TRAP) staining and dynamic fluorescent bone labeling—For bone histomorphometry, femurs were isolated from 3-month-old mice, fixed overnight in 10% PBF, dehydrated with ethanol, defatted with xylene, and embedded in methyl methacrylate (MMA) (Sigma, St. Louis, MO). Adjacent sections (5 or 10 μm in thickness) were cut and mounted on gelatin-coated slides for different staining procedures. Bone images were acquired by Zeiss AXIO Imager M1 Microscope with an automated stage and analyzed using BioQuant computer stations with BioQuant OSTEO 2009 software (Version 9.00, BIOQUANT Image Analysis Co., Nashville, TN). The region of interest starts ≈ 150 μm below the femoral growth plate, extends 1 mm distally, and flanks the two sides that are 100 μm apart from cortical bone. Three sections (≈50-100 μm apart) from each bone sample were analyzed per stain, and averages were reported. The terminology and units used are those recommended by the Histomorphometry Nomenclature Committee of the American Society for Bone and Mineral Research (37). VK staining was performed to detect the phosphate-containing minerals and calculate static bone parameters: Tb.TV, Tb.N, and Tb.Sp. To quantify structural parameters of unmineralized osteoid and osteoclast (OC)-positive resorbing surface, sections were stained with Goldner trichrome and TRAP staining solutions, respectively. The deduced indices include osteoid volume (OV), OV/BV, osteoid surface (OS), OS/BS, osteoid thickness (Mean O.Th), ratios of O.Th/Tb.Th, erosion surface (ES), ES/BS, N.Oc/BS and N.Oc/ES. For dynamic bone formation indices, mice were injected with calcein (15 mg/kg body wt.) and demeclocycline (15 mg/kg body wt.) 7 and 2 days before sample collection, respectively. Unstained MMA-embedded bone sections were obtained as described above and used to quantify mineralizing surface (MS), MS/BS, mineral apposition rate (MAR), and bone formation rate per bone surface (BFR/BS).

Ex vivo PTH secretion in intact PTGs—Two PTGs from each mouse were dissected free of surrounding thyroid and connective tissues and submerged in a micro-droplet (10 μl) of secretion medium [SM, MEM Eagles with Earle's balanced salts supplemented with 0.5 mM Mg, 0.2% bovine serum albumin, and 20 mM HEPES (pH 7.4)] placed in the center of a 13 mm track-etched (0.1 μM pore) polycarbonate (PC) membrane, floating on a large drop (0.5 ml) of ice-cold SM supplemented with 3.0 mM Ca^{2+}. Once all the glands in a given experiment were dissected out, the PC membranes carrying the glands were transferred onto fresh drops of 37 °C SM containing 0.5 mM Ca^{2+} and allowed to equilibrate for ~45 min. Experiments were then started by transferring the membrane with each pair of glands onto a fresh drop (500 μl) of SM at 37 °C containing 0.5 mM Ca^{2+} and incubating the glands for 60 min with a medium change midway (at 30 minutes). Each pair of glands was sequentially exposed to media containing increasing [Ca^{2+}] from 0.5 to 3.0 mM as described above. PTH released into the culture media was determined by ELISA and used to calculate the rate of PTH release (^{PTH}R, pg/30 min/gland). For Ca^{2+} set-points, rates of PTH release were normalized to the rate at 0.5 mM Ca^{2+} and plotted against the [Ca^{2+}], and the set-points were deduced from the curve as the [Ca^{2+}] which inhibits 50% of the Ca^{2+}-suppressible PTH release (38). Each experiment was completed in 7-8 hours. During that time, PTH release was stable and remained suppressible by high [Ca^{2+}] (Figure S1B). Medium samples from these incubations were assayed in duplicate. At the end of the experiment, the glands were collected in a RIPA buffer [in mM: 20 Tris-HCl (pH 7.5) 150 NaCl, 1 Na_2EDTA, 1 EGTA plus 1% triton X and 1% sodium deoxycholate] plus Complete© Protease Inhibitor

cocktail (Roche Applied Science, Indianapolis, IN). Gland lysates were assayed by a BCA Protein Assay Kit (Thermo Fisher Scientific, Rockford, IL) for quantification of protein content and immunoblotted for CaSR protein expression as described (32).

Statistics—Data from 2 groups were represented as mean ± the standard error of the mean (SEM) and compared using unpaired Student's t test. Significance was assigned for $p<0.05$.

Results

Age and sex affect the mineral and hormonal phenotype of control and ^{PTG}CaSR(+/−) mice

We first studied heterozygous PTG-specific *Casr* knockout [^{PTG}CaSR(+/−) or Het-KO] mice and control littermates [CaSR$^{flox/flox}$ and/or ^{PTH}Cre(+/−)] to determine the impact of sex and age on levels of serum intact PTH (sPTH), total calcium (sCa), 1,25-D (s1,25-D), and phosphate (sPi).

Effects in control mice—sPTH was 133.3±13.7 and 119.8±14.9 pg/ml in male and female control (Cont) mice, respectively, at 2 months of age (Figure 1, □). In both sexes, sPTH rose by 50 to 60% at 6 and 12 months of age ($p<0.05$) vs 2 months of age (Figure 1, □). This was accompanied by a slight decrease in sCa levels over time with levels in control mice falling from 11.1 (at 2 months of age) to 9.8 mg/dl (at 12 months of age) in males and from 10.2 (at 2 months of age) to 9.4 mg/dl (at 12 months of age) in females (Figure 1, □). We observed no changes in serum albumin levels with age or sex (data not shown), suggesting that changes in total sCa were reflecting changes in ionized [Ca^{2+}]. There were no differences in renal function with age in these mice, as assessed by serum levels of creatinine (data not shown).

s1,25-D levels in control mice showed striking sex- and age-dependent patterns. In males, s1,25-D levels were 140.0± 9.2 pmol/l in 1-month-old mice and increased by ≈100 and 200% at 6 and 12 months of age, respectively (Figure 1, □; $p < 0.01$). In female control mice, s1,25-D levels were 192.7± 21.8 pmol/l at 1 month of age, increased only by ≈30 and 70% at 3 and 6 months of age (Figure 1, □; $p < 0.01$), respectively, but then declined at 12 months of age to the levels seen in 1-month-old mice. Thus, by 6 months of age, s1,25-D levels gradually increased in both male and female control mice, corresponding to their age-dependent increases in sPTH levels. However, the effects of PTH on s1,25-D levels were significantly blunted in the 12-month-old control females, but not in males, suggesting the early development of resistance to 1-hydroxylation by Cyp27b1 in response to PTH in the aging female mice.

Effects in ^{PTG}CaSR(+/−) mice—Reducing CaSR expression in the PTGs of ^{PTG}CaSR(+/−) mice of either sex (Figure S1C) increased sPTH levels as early as 2 weeks of age, as previously reported (32), and at all time-points studied (Figure 1, ■), compared to controls (Figure 1, □; $p <0.01$). The severity of HPT was mild at 2-3 months of age, worsened with age, and was greatest in 12-month-old female ^{PTG}CaSR(+/−) mice who showed 3-fold higher sPTH levels than those of control mice (Figure 1, ■ vs □). The more severe HPT in aging female vs male mice indicates sex divergence in the presentation of the disease.

Owing to the elevated sPTH levels, sCa levels were significantly higher (by 5-10%) in the Het-KO vs control mice ($p<0.05$) at all time points, regardless of sex (Figure 1, ■ vs □). Similar to the trend seen in the control mice, sCa levels in ^{PTG}CaSR(+/−) mice were significantly lower ($p<0.05$) at 12 months of age, compared to earlier time-points (Figure 1, ■), despite their much higher sPTH levels. This indicates the development of age-induced resistance of target tissues to the calcemic actions of PTH in both control and KO mice. The

decreasing sCa could at least in part contribute to greater levels of PTH secretion in the aging control and ^{PTG}CaSR(+/−) mice.

The effects of the higher sPTH levels on s1,25-D were also age- and sex-dependent in KO mice. In male ^{PTG}CaSR(+/−) mice, s1,25-D levels were comparable to those in control mice at 1 month of age, but they were ≈2 fold higher than control mice at 3 and 6 months of age. At 12 months of age, s1,25-D levels were indistinguishable in male ^{PTG}CaSR(+/−) vs control mice (Figure 1, ■ vs □). Similar age-dependent changes in s1,25-D levels were seen in female ^{PTG}CaSR(+/−) vs control mice (Figure 1, ■ vs □). Two observations indicate sex divergence in 1,25-D metabolism and/or action in control and ^{PTG}CaSR(+/−) mice. (1) Control female mice had higher s1,25-D levels at 1, 3, and 6 months of age ($p<0.05$) vs males, but male mice had higher 1,25-D levels at 12 months of age. (2) In the ^{PTG}CaSR(+/−) mice, females had lower overall 1,25-D responses to their HPT (~20 to 30% above control females) vs males (~80- to 90% above control males) at 3- and 6-months of age (Figure 1, ■ vs □). These observations support the influence of age and sex in setting 1,25-D levels.

An important factor that could be influencing 1,25-D is sPi. We observed both age- and sex-dependent differences in this parameter. sPi levels decreased significantly ($p<0.05$) in male control mice from 2 to 12 months of age (Figure 1, □). This was not seen in control female mice. Male ^{PTG}CaSR(+/−) mice had lower sPi levels at all time-points vs control mice (Figure 1, ■ vs □) -- the expected effect of high sPTH levels to promote renal Pi excretion. Female ^{PTG}CaSR(+/−) mice, however, showed no differences in sPi levels compared to control females, indicating a male-specific hypophosphatemic effect of HPT (Figure 1, ■ vs □). Taken together, these biochemical data demonstrate the effects of age and sex on the mineral and hormonal profiles in both control and ^{PTG}CaSR(+/−) mice.

PTH secretion from glands *ex vivo* responds to different concentrations of Ca^{2+}

We developed a novel organ culture system to test the hypothesis that age- and sex-dependent changes in steady-state sPTH levels in ^{PTG}CaSR(+/−) vs control mice reflect the altered secretory capacity and sensitivity of their PTGs to $[Ca^{2+}]_e$. Micro-dissected PTGs from the mice (Figure S1A) were used to assess responsiveness of PTH release to acute, short-term changes in $[Ca^{2+}]_e$ and the expression of CaSR protein. PTH was released tonically from the cultured glands for ≥ 10 hours in vitro, and rates of PTH release (^{PTH}R, pg/30 min/gland) were suppressible by high $[Ca^{2+}] \geq 1.5$ mM over this time-period (Figure S1B).

We confirmed that the CaSR is responsible for the sensitivity of PTH release to extracellular Ca^{2+} in PTGs by comparing PTH secretion in glands isolated from 2-week-old homozygous [^{PTG}CaSR(−/−)] and heterozygous [^{PTG}CaSR(+/−)] knockout and control mice at different $[Ca^{2+}]$ from 0.5 to 3.0 mM (Figure S1). Western blotting confirmed reduced expression of CaSR protein by ≈50 and >95% in PTGs from ^{PTG}CaSR(+/−) and ^{PTG}CaSR(−/−) mice, respectively, compared to control mice (Figure S1C). The maximal PTH release (^{PTH}R-max), which was achieved at 0.75 or 1.0 mM Ca^{2+} in PTGs from female control, ^{PTG}CaSR(+/−), and ^{PTG}CaSR(−/−) mice, was 310 ± 56, 495 ± 85, and 677 ± 56 pg/30min/gland, respectively (Figure S1D). There is an inverse relationship between CaSR expression and the maximal secretory capacity of the PTGs at this age. As anticipated, there was no significant inhibition of PTH release by high $[Ca^{2+}]_e$ in PTGs from ^{PTG}CaSR(−/−) mice (Figure S1D). However, in PTGs from control and ^{PTG}CaSR(+/−) mice, maximal inhibition of PTH secretion was achieved at 2-3 mM Ca^{2+} with a minimal rate of PTH release (^{PTH}R-min) of 42.4 ± 9.6 and 55.8 ± 9.2 pg/30 min/gland, respectively (Figure S1D), confirming the role of the CaSR in mediating extracellular Ca^{2+} sensing by the PTGs. ^{PTH}R-min, which represents a Ca^{2+}-nonsuppressible pool of PTH (≈10% of the total PTH secreted), was not changed by deleting one *Casr* allele at this age.

We compared the responsiveness of PTGs to Ca^{2+} by calculating the set-point for PTH release, defined as the $[Ca^{2+}]_e$ needed to inhibit 50% of Ca^{2+}-regulated PTH secretion (38). There was a significant ($p<0.05$) right-shift in the Ca^{2+} set-point (Figure S1E) from 1.22 ± 0.03 mM in female control to 1.42 ± 0.03 mM in female ^{PTG}CaSR(+/−) PTGs (Figure S1E), confirming blunted Ca^{2+}-sensing due to reduced CaSR expression.

We next compared ^{PTH}R-max, ^{PTH}R-min, and Ca^{2+} set-points in 3- and 12-month-old male and female PTGs. In male and female control PTGs, ^{PTH}R-max values were 309 ± 28 and 518 ± 119 pg/30 min/gland at 3 months of age, respectively, and significantly increased to 588 ± 158 and 733 ± 181 pg/30 min/gland at 12 months of age, respectively ($p<0.05$ for both), without significant changes in ^{PTH}R-min values (Figures 2A, 2C). These results indicate that PTGs from female control mice release more PTH at low $[Ca^{2+}]_e$ than male control mice and that advancing age increases the magnitude of PTH released by PTGs from mice of both sexes (Figures 2A, 2C). This is at least partly due to increased gland size with age (Figure S2A). However, only age, and not sex, impacted the Ca^{2+} set-point in the control mice. The Ca^{2+} set-points for 3-month-old male and female control glands were 1.19 ± 0.03 and 1.24 ± 0.02 mM, respectively, which significantly shifted to the left ($p<0.05$) to 1.07 ± 0.03 and 1.04 ± 0.04 mM at 12 months of age (Figures 2B, 2C). This surprising left-shift of the Ca^{2+} set-point was due to greater CaSR expression in aging mice, as demonstrated by Western blotting of gland lysates from 12- vs 3-month-old female control mice (Figure S2B, S2C). This supports the idea that aging PTGs may adapt to changes in mineral homeostasis by enhancing their Ca^{2+}-sensing through increased CaSR expression.

CaSR haploinsufficiency caused a significant right-shift in the Ca^{2+} set-point in ^{PTG}CaSR(+/−) vs control PTGs of either sex that was noted at both early and later ages (Figures 2B, 2C). There was, however, a sex-based difference in the degree of the shift in the Ca^{2+} set-point at 3 months of age [in males: from 1.19 ± 0.03 in control to 1.39 ± 0.02 mM in ^{PTG}CaSR(+/−) mice ($\Delta = 0.20$ mM; $p<0.01$); in females: from 1.24 ± 0.02 in control to 1.53 ± 0.04 mM in ^{PTG}CaSR(+/−) mice ($\Delta = 0.29$ mM; $p<0.01$)] and also at 12 months of age [in males: from 1.07 ± 0.03 in control to 1.22 ± 0.02 mM in ^{PTG}CaSR(+/−) mice ($\Delta = 0.15$ mM; $p<0.01$); in females: from 1.04 ± 0.04 in control to 1.30 ± 0.03 mM in ^{PTG}CaSR(+/−) mice ($\Delta = 0.26$ mM; $p<0.01$)] (Figures 2B, 2C). Thus, CaSR haploinsufficiency has a greater impact on the responses of the PTGs in female vs male mice to changes in the $[Ca^{2+}]_e$ -- manifested by greater right-shifts in Ca^{2+} set-points in PTGs from female mice.

We also observed a left-shift of the Ca^{2+} set-point in the PTGs from ^{PTG}CaSR(+/−) at 12 vs 3 months of age (Figures 2B, 2C), as seen in the control mice, indicating that an age-dependent adaptive response of PTGs to chronic HPT also occurred in these mice. Similarly, increased CaSR expression is likely the underlying mechanism enhancing the sensitivity to extracellular Ca^{2+} in the glands from aging ^{PTG}CaSR(+/−) mice, and this was demonstrated by Western blotting (Figure S2B, S2C). However, the limited ability of 12-month-old ^{PTG}CaSR(+/−) PTGs to increase CaSR expression (due to deletion of one *Casr* allele) prevented the restoration of Ca^{2+} set-points into the normal range, especially in the females. This inadequate compensation by the PTGs may underlie the more profound HPT of the female ^{PTG}CaSR(+/−) mice.

Heterozygous knockout of the CaSR in PTGs also impacted the ^{PTH}R-max and ^{PTH}R-min in a sex- and age-dependent manner (Figures 2A, 2C). At 3 months of age, ^{PTH}R-max significantly increased by ≈60% from 309 ± 28 pg/30min/gland in male control PTGs to 498 ± 110 pg/30min/gland in male ^{PTG}CaSR(+/−) mice ($p<0.05$), but there was no significant difference in this parameter between female control vs ^{PTG}CaSR(+/−) mice (518 ± 119 vs 553 ± 107 pg/30min/gland) (Figures 2A, 2C). In PTGs from 12-month-old mice, ^{PTH}R-max was significantly increased by >90% assessed in ^{PTG}CaSR(+/−) mice of both sexes [male:

1197 ± 320 pg/30min/gland; female: 1282 ± 279 pg/30min/gland] compared to control mice [male: 588 ± 158 pg/30min/gland; female: 733 ± 181 pg/30min/gland] ($p<0.05$) (Figures 2A, 2C). These data suggest that in the oldest mice studied (12 months) there was an increase in the maximal secretory capacity of the PTGs (seen under low Ca^{2+} conditions), but this was accompanied by enhanced sensitivity of the PTGs to $[Ca^{2+}]_e$. However, these effects of aging were more evident in ^{PTG}CaSR(+/−) mice (Figures 2A, 2C), in which deletion of one *Casr* allele is predicted to impede putative aging-induced adaptive/feedback responses of the PTGs.

Age affects kidney and intestinal epithelial responses to HPT in ^{PTG}CaSR(+/−) mice

The decreasing s1,25-D and sCa levels, despite higher sPTH levels, in the 12-month-old ^{PTG}CaSR(+/−) mice (Figure 1), prompted us to determine whether target organs of PTH and 1,25-D developed resistance to these hormones' actions with age and whether this altered expression of genes important in Ca^{2+} transport and in PTH- and 1,25-D-mediated actions in these tissues. We performed qPCR on RNA from the kidneys and duodenal epithelia from 3- and 12-month-old ^{PTG}CaSR(+/−) and control mice. Levels of mRNA for Cyp27b1, TRPV5, and CaSR -- genes whose expression is promoted by acute and long-term infusions of PTH in previous studies in rat and mouse models (4,9,40) -- were significantly ($p<0.01$) increased by ≈300, 200, and 30%, respectively, in the kidneys of 3-month old ^{PTG}CaSR(+/−) vs control mice of both sexes (Figure 3A, ■ vs □). The increased renal Cyp27b1 mRNA expression is consistent with the observation of elevated s1,25-D levels in 3-month-old ^{PTG}CaSR(+/−) vs control mice (Figure 1, ■ vs □) as well as the increased RNA levels of the VDR, TRPV6, CalB, and PMCA in the duodenal epithelium (Figure 3B, ■ vs □). These changes in gene expression could be mediating the hypercalcemia of ^{PTG}CaSR(+/−) mice. In contrast, these HPT-induced changes in gene expression were blunted in the kidney and intestinal epithelium of 12-month-old ^{PTG}CaSR(+/−) mice (Figure 3A, ■ vs □). Furthermore, the ability of high PTH to increase Cyp24A1 expression in the kidneys of 3-month-old ^{PTG}CaSR(+/−) mice was also blunted in 12-month-old mice, suggesting that reduced s1,25-D in aging mice was not due to increased renal catabolism (Figure 3A). These data together confirm target organ resistance to HPT that developed with aging in these mice. Such resistance could be mediated by reduced expression of the PTH 1 receptor (PTH1R) in the kidney, supported by a >60% reduction in PTH1R RNA in kidneys from 12-month-old vs 3-month-old ^{PTG}CaSR(+/−) mice (Figure 3A).

Age and sex alter the skeletal responses to HPT

Skeletal effects of HPT in humans have been described as catabolic or anabolic depending on the site examined, the severity of hypersecretion, and the age and sex of the patients (41-45). To define the contribution of some of these factors to skeletal features of HPT, we performed microcomputed tomography (μCT) and histomorphometry on both trabecular (Tb) and cortical (Ct) bone in male and female control and ^{PTG}CaSR(+/−) mice at different ages.

Properties of Tb bone by μCT in the distal femur—In control mice of both sexes, maximal overall bone size, indicated by Tb tissue volume (Tb.TV), and peak bone mass, indicated by Tb bone fraction (Tb.BV/TV), were achieved at ≈2-3 months of age (Figures 4B, 4D, □). While Tb.TV was stably maintained thereafter through 12 months of age, Tb.BV/TV declined significantly at 12 months of age in male control mice and earlier at 6 and 12 months of age in female control mice, as demonstrated by the 3-D reconstructed μCT images (Figures 4A, 4C, Cont) and their quantifications (Figures 4B, 4D, □). At 12 months of age, only ≈30% and 15% of Tb.BV/TV remained in the male and female control mice, respectively (Figures 4A, 4C, Cont; 4B, 4D, □). Associated with the low Tb.BV/TV values in aging control mice of both sexes were progressive decreases in Tb number (Tb.N) and

connectivity density (Tb.CD) and increases in Tb thickness (Tb.Th) and spacing (Tb.Sp) (Figures 4B, 4D, □). During skeletal remodeling at younger ages (2-6 months), increasing Tb.Th appeared to compensate for the decreasing Tb.N to maintain a stable level of bone mass (Tb.BV/TV) in control mice (Figures 4B, 4D, □). This compensatory effect was, however, insufficient at ≥6 months (females) and 12 months of age (males), since Tb.BV/TV fell significantly at those ages (Figures 4B, 4D). These data also indicate sex differences in bone remodeling under normal physiological conditions with early Tb loss in the females.

The impact of HPT (due to CaSR KO in PTGs) on Tb bone was also age- and sex-dependent. In male ^{PTG}CaSR(+/−) mice at 2 months of age, Tb.BV/TV and other structural parameters were equivalent to those of control mice, but skeletal anabolic effects -- increased Tb.BV/TV and Tb.CD and reduced Tb.Sp -- emerged in male ^{PTG}CaSR(+/−) mice at 3 months of age and persisted throughout the time-points tested (Figures 4A, Cont vs Het-KO; Figures 4B; ■ vs □). The anabolic effects of HPT on bone were reflected in increased Tb.N and not in changes in Tb.Th (Figures 4B; ■ vs □).

As opposed to the anabolic effects of HPT on Tb bone in male mice, catabolic effects -- decreased Tb.BV/TV, Tb.CD, Tb.N, and Tb.Th and increased Tb.Sp -- were seen in 2- and 3-month-old female ^{PTG}CaSR(+/−) vs control mice (Figures 4C: Cont vs Het-KO; 4D; ■ vs □). At 6 months of age, all Tb parameters were indistinguishable between female ^{PTG}CaSR(+/−) and control mice (Figures 4D; ■ vs □). Interestingly, we could only uncover a putative anabolic effect of HPT on female Tb bone at 12 months of age (Figures 4C; Cont vs Het-KO, 4D; ■ vs □). We viewed this as possibly due to the summation of dynamic aging-related and HPT-related changes in Tb bone turnover. Like in male mice, both catabolic and anabolic actions of HPT on female Tb bone were associated with changes in Tb.N, but not in Tb.Th (Figures 4D; ■ vs □), suggesting that HPT has greater impact on the number of bone forming/resorbing units than the cellular activity in those units.

Tb bone properties by static and dynamic histomorphometry—To explore the underlying mechanisms of the sex-specific actions of HPT on Tb bone, we performed histomorphometry on distal femurs of 3-month-old mice. Consistent with the μCT data, male ^{PTG}CaSR(+/−) mice showed increased Tb.BV/TV and Tb.N and decreased Tb.Sp in von Kossa-stained bone sections compared to control bone (Figures 5A, 5B; ■ vs □). In contrast, the opposite effects were seen in bone from female ^{PTG}CaSR(+/−) vs control mice (Figures 5A, 5B; ■ vs □). By Goldner staining, there were no differences in osteoid content in male ^{PTG}CaSR(+/−) vs control Tb bone, as indicated by comparable ratios of osteoid volume/BV (OV/BV), osteoid surface/bone surface (OS/BS), and osteoid thickness/Tb.Th (O.Th/Tb.Th) (Figures 5C, 5D; ■ vs □). On the other hand, OV/BV, OS/BS, and O.Th/Tb.Th were all increased in the female Het-KO vs control Tb bones (Figures 5C, 5D; ■ vs □).

To determine whether increased production of unmineralized matrix and/or a delay in matrix mineralization were causing the osteoid accumulation in bone from female ^{PTG}CaSR(+/−) mice, we measured dynamic bone formation parameters by dual-fluorescent calcein/demecylocycline labeling. Increased mineral apposition rates (MARs) in bones from female ^{PTG}CaSR(+/−) vs control mice (Figures 5E, 5F; ■ vs □) indicate that matrix synthesis must increase and exceed the MAR to cause osteoid accumulation in the female ^{PTG}CaSR(+/−) mice. However, overall bone formation rate per BS (BFR/BS) was not changed in these bones, due to a decreased proportion of mineralizing surface (MS) over BS (MS/BS) (Figures 5E, 5F; ■ vs □). Thus, female ^{PTG}CaSR(+/−) mice also appeared to show this defect in achieving full mineralization of the matrix, despite their higher level of synthesis vs control mice.

Histomorphometry in male mice provided an important contrast. MS/BS and BFR/BS were significantly decreased, but MAR was unchanged in bone from male ^{PTG}CaSR(+/−) vs control mice (Figures 5E, 5F; ■ vs □), indicating a state of reduced bone turnover. This notion is further supported by decreased % erosion surface over bone surface (ES/BS), reduced number of osteoclasts residing on the erosion surface (Oc.N/ES), and a decrease in the overall Oc.N per BS (Oc.N/BS) in bone from male ^{PTG}CaSR(+/−) vs control mice by tartrate-resistant acid phosphatase (TRAP) staining of OCs (Figures 5G, 5H, ■ vs □). These data indicate reduced OC activity in the Tb bone of male ^{PTG}CaSR(+/−) mice. This contrasts strongly with the increased bone turnover in female ^{PTG}CaSR(+/−) mice and enhanced OC activities, as indicated by increased Oc.N/ES without altering the ES/BS ratio (Figures 5G, 5H; ■ vs □).

Ct bone properties in the tibio-fibular junction—To examine responses of Ct bone to HPT, we performed μCT analyses of bones from control and ^{PTG}CaSR(+/−) mice. In control and ^{PTG}CaSR(+/−) mice of both sexes, the overall bone size, indicated by Ct tissue volume (Ct.TV) (including both bone and marrow volume), continuously increased from 3 to 12 months of age by up to 30% (Figures 6A, 6B, 6E, 6F). Although Ct.Th also increased with age, overall Ct bone fraction (Ct.BV/TV) was reduced in males or unchanged in females (Figures 6A, 6B, 6E, 6F), due to a disproportionate increase in bone marrow volumes (data not shown).

Ct bone in male and female mice matured with age, as indicated by increasing hydroxyapatite (HA) content in the bone. To quantify these changes, we segregated 2 different fractions of bone by μCT: low density bone (LDB) defined as 420-1400 mg HA/mm^3 and high density bone (HDB) defined as >1400 mg HA/mm^3 (Figures 6C, 6D, 6G, 6H). In bones from either control or ^{PTG}CaSR(+/−) mice regardless of sex, LDB fractions significantly decreased from 70-75% at 3 months to 25-30% at 12 months of age. In contrast, the fraction of HDB, which originates in the middle of Ct bone (Figures 6C, 6G), increased from ≈15-25% at 3 months to ≈70% at 12 months of age (Figures 6C, 6D, 6G, 6H).

The LDB fraction tended to increase in male ^{PTG}CaSR(+/−) mice at 3 months and became significantly greater at 6, 9 and 12 months of age vs controls. HDB fractions in male ^{PTG}CaSR(+/−) mice were markedly lower, however, than those in control mice at all time-points (Figure 6D, ■ vs □). In male control mice at 12 months of age, LDB generally resided in thin concentric matrix layers adjacent to either periosteum or endosteum of the Ct bone (Figure 6C). In bones from male ^{PTG}CaSR(+/−) mice of the same age, the increased amount of LDB seemed to aggregate preferentially around the endosteum (Figure 6C).

The impact of HPT on female Ct bone was milder and changed biphasically with age. At 3 months of age, LDB fraction was significantly lower while the HDB fraction was significantly higher in the Ct bone of female ^{PTG}CaSR(+/−) vs control mice (Figures 6G; 6H, ■ vs □). In contrast, this trend was reversed -- increased LDB and decreased HBD fractions -- at 12 months of age (Figures 6G; 6H, ■ vs □). The increased amount of LDB also aggregated around the endosteum in the 12-month-old female ^{PTG}CaSR(+/−) mice (Figure 6G). These Ct bone data, together with those on Tb bone, support sex- and age-dependent effects on the site-specific skeletal responses to HPT. In male Het-KO mice, HPT spared Tb bone from the natural age-dependent decrements, but not Ct bone, which showed delayed bone mineralization. In contrast, in females, HPT increased Tb bone turnover, which caused bone loss at early age, but there was preservation of the architecture of Ct bone. However, in aging female Het-KO mice, HPT produced anabolic effects on Tb bone and catabolic effects on Ct bone, similar to those seen in male counterparts.

Discussion

Neonatal onset of HPT in our ^{PTG}CaSR(+/−) mouse model permitted study of the progressive effects of hormone excess across a broad spectrum of age, not previously studied. Tissue-specific targeting of gene deletion in this model preserved CaSR functions in tissues outside the PTGs, allowing for responses of target organs to changes in sCa levels to be expressed which is not possible in global CaSR knockouts (31). The biochemical, hormonal, and skeletal manifestations of HPT in our mice, which resemble the presentation of mild HPT in humans, were assessed on a stable genetic background and defined diet and under controlled environmental conditions. These variables cannot be held constant in human studies. This model allows us to understand the evolving phenotype of HPT in males and females through skeletal maturation and aging and should also be valuable for testing new approaches to control PTH hypersecretion and modify disease progression.

Our studies of PTGs in culture may shed light on the mechanisms predisposing postmenopausal women and elderly patients to develop HPT. Sex-based differences in secretory responses and CaSR expression in PTGs isolated from 3- vs 12-month-old control and ^{PTG}CaSR(+/−) mice, highlight a central role for the CaSR in the development of HPT. The increased CaSR protein expression and left-shifted Ca^{2+} set-points for PTH secretion in aging glands of both genotypes indicate a novel adaptation by the PTGs to modulate PTH secretion in an effort perhaps to prevent the development of HPT with aging. This adaptation seems to require both *Casr* alleles based on the following notions. (1) Our ^{PTG}CaSR(+/−) mice develop much greater degrees of PTH hypersecretion at later ages, as their glands adapt less to aging than controls. (2) Tumors from patients with HPT have reduced CaSR expression. This may prevent such PTGs from regulating external demands for the control of PTH secretion and cell proliferation due to aging, thus fueling the development of HPT.

There was a consistently larger impact of CaSR deletion on HPT in female vs male ^{PTG}CaSR (+/−) mice. This was evident by greater right shifts in Ca^{2+} set-points in PTGs from female KO mice. Consequently, the aging-mediated adaptation of their PTGs (i.e., increased CaSR expression and left-shift in Ca^{2+}-setpoint) could not completely compensate to move the set-points into a normal range. Furthermore, PTGs from female mice have larger secretory capacities and bigger Ca^{2+}-non-suppressible pools of PTH than their male counterparts, as reflected in greater ^{PTH}R-max and ^{PTH}R-min values, respectively, in both control and ^{PTG}CaSR(+/−) mice. These intrinsic differences in the PTGs, based on sex, if borne out in human studies, could begin to explain the predisposition for women to develop primary HPT -- given the right genetic, nutritional, or hormonal triggers.

How does aging alter calciotropic hormones and/or their actions to exacerbate PTH hypersecretion in ^{PTG}CaSR(+/−) mice? The concurrent decreases in sCa and increasing sPTH levels with aging over 12 months in both control and ^{PTG}CaSR(+/−) mice indicate waning calcemic effects of PTH. This is likely due to development of target organ resistance to the hormone, as demonstrated by unresponsiveness of renal Cyp27b1 and TRPV5 and several intestinal Ca^{2+}-transport genes to high PTH levels. Consistent with the decreased renal responses, s1,25-D levels decreased in 12-month-old ^{PTG}CaSR(+/−) and control mice (compared to younger counterparts), leading to lowering of sCa. In response to this negative Ca^{2+} balance, control mice increased sPTH and s1,25-D levels and reset their sCa to lower levels perhaps in an effort to maintain mineral homeostasis and preserve skeletal mass. However, in Casr haploinsufficient ^{PTG}CaSR(+/−) mice, the blunting of these feedback responses augmented their PTH hypersecretion and the presentation of HPT. Our gene expression data suggest that the decreased renal expression of PTH1R RNA could contribute

to the renal resistance to PTH in aging control and ^{PTG}CaSR(+/−) mice. Together, our studies support the concept that aging-induced target organ resistance is a major contributor to the promotion of HPT -- particularly in mice with insufficient CaSR reserve in their PTGs to upregulate that gene and modulate PTH secretion. The pathways that mediate what we have termed “adaptation” of the PTGs to aging are unknown, but could involve the VDR, 1,25-D, and other hormones and factors [e.g., fibroblast growth factor 23 (FGF23), insulin growth factor 1, klotho, etc]. More importantly, how sex-based factors alter responsiveness of PTG and other target organs to changes in mineral and hormonal status remains a critical issue to address.

Bone mass and structure change substantially with age. In control mice of both sexes, Tb bone decreased progressively with age, mainly due to decreased Tb.N, suggesting a possible decrease in stem cell recruitment to bone forming cells. Although, Tb.Th increased (by ≈30-40%) with age and helped maintain the overall bone mass at early time points (3 and 6 months), by 12 months of age, the majority of Tb bone was lost in control mice. These changes in Tb bone occurred concurrently with increases in the size, thickness, and more importantly mineral content of Ct bone, indicating a redistribution of mineral from Tb to Ct bone with age. This may help to preserve overall bone strength and mechanical properties as these profound changes in Tb elements occur. However, the loss of high-turnover Tb bone may contribute to the reduced calcemic actions of PTH in aging mice. Age-dependent changes in skeletal parameters are undoubtedly multifactorial. Changes in sPTH, sCa, s1,25-D, gonadal steroids and growth factors with as well as bone cell senescence could all be contributing. Furthermore, altered end-organ (i.e., bone) responsiveness to the actions of PTH, Ca, and 1,25-D could also be involved.

We observed profound sex differences in the skeletal responses to chronic HPT. In male ^{PTG}CaSR(+/−) mice, Tb bone mass was preserved or increased, compared to control mice, due to an increased Tb.N. This could be due to increased stem cell recruitment due to chronically high PTH levels (47). Tb bone changes in the male ^{PTG}CaSR(+/−) mice were accompanied by delayed maturation of Ct bone, as indicated by unchanged Ct.Th with age, and a delay in the transition of LDB to HDB in the cortex. μCT analyses further demonstrated that delayed matrix mineralization mainly occurred around the endosteum. It appears that chronic HPT may preserve Tb bone at the expense of Ct bone integrity. This has been observed in cross-sectional cohorts of humans with primary HPT (41-45).

The skeletal responses to chronic HPT are more complex in female ^{PTG}CaSR(+/−) mice. High sPTH actually reduced Tb bone mass in female ^{PTG}CaSR(+/−) mice and increased mineral content in their Ct bone earlier -- at 2 and 3 months of age. Chronic HPT had no apparent impact on Tb and Ct bone parameters at 6 and 9 months of age and produced modest anabolic effects in Tb bone and catabolic effects in Ct bone in 12-month-old female ^{PTG}CaSR(+/−) mice. These age-dependent changes in the effects of PTH on bone have not been previously appreciated, but could have clinical relevance in terms of disease management.

Sex differences in the skeletal responses to HPT were reinforced by histomorphometric analyses of static and dynamic parameters in Tb bone at 3 months of age. We found that HPT *reduced bone turnover* in male ^{PTG}CaSR(+/−) mice and *promoted turnover* in female counterparts. Bone anabolic effects in the males were mainly due to the reduced ES and Oc.N in the resorbing pits. In contrast, HPT produced catabolic effects in female mice by increasing Oc.N in the resorbing pits. Furthermore, the increased bone turnover might have caused an imbalance between bone matrix synthesis and its mineralization (i.e., matrix production outpacing mineralizing activity of bone cells), leading to an excess of unmineralized osteoid on the trabecular bone surface in the female ^{PTG}CaSR(+/−) mice. Our

observations in female Tb bones are in line with the general view that PTH increases bone turnover, resorption, and dermineralization. Our observations in male mice, however, suggest that PTH exerts the opposite effect in males. It is conceivable that skeletal actions of PTH are clearly modified by other critical sex-specific factors such as gonadal steroids. Other sex-based differences in mineral and hormonal states could be involved. CaSRs and VDRs are co-expressed in many target cells of PTH, including bone cell populations, and exert critical functions in them (32). Through their signaling pathways, changes in the sCa and s1-25-D levels could also contribute to the different skeletal responses we observed. HPT could also mediate mineral and hormonal changes through direct actions of PTH on bone. For example, high PTH could mediate sustained hypercalcemia by maintaining Tb bone, which has faster turnover than Ct bone. Future studies are required to understand these relationships.

In summary, this model of early onset mild HPT allowed us to uncover changes in PTG function and in PTH and 1,25-D actions with aging heretofore unexpected. Detailed PTH secretory responses in a novel culture system and skeletal assessments by uCT provide new insights into PTG function and changes in Tb and Ct bone compartments in male and female mice. These findings may explain many clinical observations. The first is the propensity for mild PTH excess to weaken Ct bone. The second is the possibility that the extent of bone resorption at the tissue level by OCs differs in male vs female bone. The third is that factors related to sex substantially modify the effects of HPT on both Tb and Ct bone and serum minerals and hormones. This model has possible translational and therapeutic applications. On a defined genetic background, one can introduce changes in dietary Ca^{2+}, P, or vitamin D or alter signaling molecules genetically -- Cyp27b1, FGF23, klotho, the PTH1R -- to define the role of these factors in the development and progression of the disease. New drugs can be directly tested for activity on PTG function.

Supplementary Material

Refer to Web version on PubMed Central for supplementary material.

Acknowledgments

This work was supported by NIH RO1-AG21353 (W.C.), R21-AR50662 (W.C.), RO1-AR56256 (C.T.), RO1-AR050023 (D.B.), RO1-AR055588 (DS), and by the Department of Veterans Affairs Merit Review (D.B.) and Program Project Award (W.C., D.B., and D.S.), and the Department of Defense-USAMRMC W81XWH-05-2-0094 (W.C. and D.S.). Wenhan Chang wrote the drafts of the manuscript along with critical input from Dolores Shoback, Chialing Tu and Daniel Bikle. Zhiqiang Cheng, Nathan Liang, Tsui-Hua Chen, Alfred Li, Christian Santa Maria, Michael You, Hanson Ho, and Fuqing Song performed all of the experiments and tissue analyses in the manuscript. All authors approved the final draft of the manuscript.

References

1. Brown EM, MacLeod RJ. Extracellular calcium sensing and extracellular calcium signaling. Physiol Rev. 2001; 81(1):239–297. [PubMed: 11152759]
2. Brown EM. The calcium-sensing receptor: physiology, pathophysiology and CaR-based therapeutics. Subcell Biochem. 2007; 45:139–67. [PubMed: 18193637]
3. Chang W, Shoback D. Extracellular Ca2+-sensing receptors--an overview. Cell Calcium. 2004; 35(3):183–96. [PubMed: 15200142]
4. van Abel M, Hoenderop JG, van der Kemp AW, Friedlaender MM, van Leeuwen JP, Bindels RJ. Coordinated control of renal Ca(2+) transport proteins by parathyroid hormone. Kidney Int. 2005; 68(4):1708–21. [PubMed: 16164647]
5. Bajwa A, Forster MN, Maiti A, Woolbright BL, Beckman MJ. Specific regulation of CYP27B1 and VDR in proximal versus distal renal cells. Arch Biochem Biophys. 2008; 477(1):33–42. [PubMed: 18593564]

6. Prosser DE, Jones G. Enzymes involved in the activation and inactivation of vitamin D. Trends Biochem Sci. 2004; 29(12):664–73. [PubMed: 15544953]
7. Brown AJ, Dusso A, Slatopolsky E, Vitamin D. Am J Physiol. 1999; 277(2 Pt 2):F157–75. [PubMed: 10444570]
8. Armbrecht HJ, Hodam TL, Boltz MA. Hormonal regulation of 25-hydroxyvitamin D3-1alpha-hydroxylase and 24-hydroxylase gene transcription in opossum kidney cells. Arch Biochem Biophys. 2003; 409(2):298–304. [PubMed: 12504896]
9. Peng JB, Brown EM, Hediger MA. Epithelial Ca2+ entry channels: transcellular Ca2+ transport and beyond. J Physiol. 2003; 551(Pt 3):729–40. [PubMed: 12869611]
10. Fleet JC, Eksir F, Hance KW, Wood RJ. Vitamin D-inducible calcium transport and gene expression in three Caco-2 cell lines. Am J Physiol Gastrointest Liver Physiol. 2002; 283(3):G618–25. [PubMed: 12181175]
11. Cai Q, Chandler JS, Wasserman RH, Kumar R, Penniston JT. Vitamin D and adaptation to dietary calcium and phosphate deficiencies increase intestinal plasma membrane calcium pump gene expression. Proc Natl Acad Sci U S A. 1993; 90(4):1345–9. [PubMed: 7679502]
12. Christakos S, Norman AW. Vitamin D-dependent calcium-binding protein synthesis by chick kidney and duodenal polysomes. Arch Biochem Biophys. 1980; 203(2):809–15. [PubMed: 7458355]
13. Lotinun S, Evans GL, Bronk JT, Bolander ME, Wronski TJ, Ritman EL, Turner RT. Continuous parathyroid hormone induces cortical porosity in the rat: effects on bone turnover and mechanical properties. J Bone Miner Res. 2004; 19(7):1165–71. [PubMed: 15177000]
14. Iida-Klein A, Lu SS, Kapadia R, Burkhart M, Moreno A, Dempster DW, Lindsay R. Short-term continuous infusion of human parathyroid hormone 1-34 fragment is catabolic with decreased trabecular connectivity density accompanied by hypercalcemia in C57BL/J6 mice. J Endocrinol. 2005; 186(3):549–57. [PubMed: 16135674]
15. Pallan S, Rahman MO, Khan AA. Diagnosis and management of primary hyperparathyroidism. BMJ. 2012; 344:e1013. [PubMed: 22431655]
16. Shlapack MA, Rizvi AA. Normocalcemic primary hyperparathyroidism-characteristics and clinical significance of an emerging entity. Am J Med Sci. 2012; 343(2):163–6. [PubMed: 22173046]
17. Gracie D, Hussain SS. Use of minimally invasive parathyroidectomy techniques in sporadic primary hyperparathyroidism: systematic review. J Laryngol Otol. 2012; 126(3):221–7. [PubMed: 22032618]
18. Salti GI, Fedorak I, Yashiro T, Fulton N, Hara H, Yousefzadeh D, Kaplan EL. Continuing evolution in the operative management of primary hyperparathyroidism. Arch Surg. 1992; 127(7): 831–6. discussion 836-7. [PubMed: 1524484]
19. Cetani F, Pardi E, Borsari S, Viacava P, Dipollina G, Cianferotti L, Ambrogini E, Gazzerro E, Colussi G, Berti P, Miccoli P, Pinchera A, Marcocci C. Genetic analyses of the HRPT2 gene in primary hyperparathyroidism: germline and somatic mutations in familial and sporadic parathyroid tumors. J Clin Endocrinol Metab. 2004; 89(11):5583–91. [PubMed: 15531515]
20. Rosenberg CL, Kim HG, Shows TB, Kronenberg HM, Arnold A. Rearrangement and overexpression of D11S287E, a candidate oncogene on chromosome 11q13 in benign parathyroid tumors. Oncogene. 1991; 6(3):449–53. [PubMed: 2011400]
21. Hsi ED, Zukerberg LR, Yang WI, Arnold A. Cyclin D1/PRAD1 expression in parathyroid adenomas: an immunohistochemical study. J Clin Endocrinol Metab. 1996; 81(5):1736–9. [PubMed: 8626826]
22. Heppner C, Kester MB, Agarwal SK, Debelenko LV, Emmert-Buck MR, Guru SC, Manickam P, Olufemi SE, Skarulis MC, Doppman JL, Alexander RH, Kim YS, Saggar SK, Lubensky IA, Zhuang Z, Liotta LA, Chandrasekharappa SC, Collins FS, Spiegel AM, Burns AL, Marx SJ. Somatic mutation of the MEN1 gene in parathyroid tumours. Nat Genet. 1997; 16(4):375–8. [PubMed: 9241276]
23. Richert L, Trombetti A, Herrmann FR, Triponez F, Meier C, Robert JH, Rizzoli R. Age and gender distribution of primary hyperparathyroidism and incidence of surgical treatment in a European country with a particularly high life expectancy. Swiss Med Wkly. 2009; 139(27-28):400–4. [PubMed: 19629768]

24. Cetani F, Picone A, Cerrai P, Vignali E, Borsari S, Pardi E, Viacava P, Naccarato AG, Miccoli P, Kifor O, Brown EM, Pinchera A, Marcocci C. Parathyroid expression of calcium-sensing receptor protein and in vivo parathyroid hormone-Ca(2+) set-point in patients with primary hyperparathyroidism. J Clin Endocrinol Metab. 2000; 85(12):4789–94. [PubMed: 11134144]
25. Farnebo F, Enberg U, Grimelius L, Backdahl M, Schalling M, Larsson C, Farnebo LO. Tumor-specific decreased expression of calcium sensing receptor messenger ribonucleic acid in sporadic primary hyperparathyroidism. J Clin Endocrinol Metab. 1997; 82(10):3481–6. [PubMed: 9329389]
26. Autry CP, Kifor O, Brown EM, Fuller FH, Rogers KV, Halloran BP. Ca2+ receptor mRNA and protein increase in the rat parathyroid gland with advancing age. J Endocrinol. 1997; 153(3):437–44. [PubMed: 9203998]
27. Peacock M. Calcium metabolism in health and disease. Clin J Am Soc Nephrol. 2010; 5(Suppl 1):S23–30. [PubMed: 20089499]
28. Marcus R, Madvig P, Young G. Age-related changes in parathyroid hormone and parathyroid hormone action in normal humans. J Clin Endocrinol Metab. 1984; 58(2):223–30. [PubMed: 6319444]
29. Eastell R, Yergey AL, Vieira NE, Cedel SL, Kumar R, Riggs BL. Interrelationship among vitamin D metabolism, true calcium absorption, parathyroid function, and age in women: evidence of an age-related intestinal resistance to 1,25-dihydroxyvitamin D action. J Bone Miner Res. 1991; 6(2): 125–32. [PubMed: 2028834]
30. Imanishi Y, Hosokawa Y, Yoshimoto K, Schipani E, Mallya S, Papanikolaou A, Kifor O, Tokura T, Sablosky M, Ledgard F, Gronowicz G, Wang TC, Schmidt EV, Hall C, Brown EM, Bronson R, Arnold A. Primary hyperparathyroidism caused by parathyroid-targeted overexpression of cyclin D1 in transgenic mice. J Clin Invest. 2001; 107(9):1093–102. [PubMed: 11342573]
31. Ho C, Conner DA, Pollak MR, Ladd DJ, Kifor O, Warren HB, Brown EM, Seidman JG, Seidman CE. A mouse model of human familial hypocalciuric hypercalcemia and neonatal severe hyperparathyroidism [see comments]. Nat Genet. 1995; 11(4):389–94. [PubMed: 7493018]
32. Chang W, Tu C, Chen TH, Bikle D, Shoback D. The extracellular calcium-sensing receptor (CaSR) is a critical modulator of skeletal development. Sci Signal. 2008; 1(35):ra1. [PubMed: 18765830]
33. Rodriguez L, Cheng Z, Chen TH, Tu C, Chang W. Extracellular calcium and parathyroid hormone-related peptide signaling modulate the pace of growth plate chondrocyte differentiation. Endocrinology. 2005; 146(11):4597–608. [PubMed: 16099862]
34. Cheng Z, Tu C, Rodriguez L, Dvorak MM, Gassmann M, Bettler B, Shoback D, Chang W. Type B gamma-aminobutyric acid receptors modulate the expression and function of the extracellular Ca2+-sensing receptor in murine growth plate chondrocytes. 2006 in presss.
35. Dvorak MM, Chen TH, Orwoll B, Garvey C, Chang W, Bikle DD, Shoback DM. Constitutive activity of the osteoblast Ca2+-sensing receptor promotes loss of cancellous bone. Endocrinology. 2007; 148(7):3156–63. [PubMed: 17412806]
36. Dvorak-Ewell MM, Chen TH, Liang N, Garvey C, Liu B, Tu C, Chang W, Bikle DD, Shoback DM. Osteoblast extracellular Ca2+ -sensing receptor regulates bone development, mineralization, and turnover. J Bone Miner Res. 2011; 26(12):2935–47. [PubMed: 21956637]
37. Parfitt AM, Drezner MK, Glorieux FH, Kanis JA, Malluche H, Meunier PJ, Ott SM, Recker RR. Bone histomorphometry: standardization of nomenclature, symbols, and units. Report of the ASBMR Histomorphometry Nomenclature Committee. J Bone Miner Res. 1987; 2(6):595–610. [PubMed: 3455637]
38. Brown EM. Four-parameter model of the sigmoidal relationship between parathyroid hormone release and extracellular calcium concentration in normal and abnormal parathyroid tissue. J Clin Endocrinol Metab. 1983; 56(3):572–81. [PubMed: 6822654]
39. Wettschureck N, Lee E, Libutti SK, Offermanns S, Robey PG, Spiegel AM. Parathyroid-specific double knockout of Gq and G11 alpha-subunits leads to a phenotype resembling germline knockout of the extracellular Ca2+ -sensing receptor. Mol Endocrinol. 2007; 21(1):274–80. [PubMed: 16988000]

40. van Abel M, Huybers S, Hoenderop JG, van der Kemp AW, van Leeuwen JP, Bindels RJ. Age-dependent alterations in Ca2+ homeostasis: role of TRPV5 and TRPV6. Am J Physiol Renal Physiol. 2006; 291(6):F1177–83. [PubMed: 16705151]

41. Bilezikian JP, Silverberg SJ, Shane E, Parisien M, Dempster DW. Characterization and evaluation of asymptomatic primary hyperparathyroidism. J Bone Miner Res. 1991; 6(Suppl 2):S85–9. discussion S121-4. [PubMed: 1662460]

42. Silverberg SJ, Gartenberg F, Jacobs TP, Shane E, Siris E, Staron RB, McMahon DJ, Bilezikian JP. Increased bone mineral density after parathyroidectomy in primary hyperparathyroidism. J Clin Endocrinol Metab. 1995; 80(3):729–34. [PubMed: 7883824]

43. Bilezikian JP, Brandi ML, Rubin M, Silverberg SJ. Primary hyperparathyroidism: new concepts in clinical, densitometric and biochemical features. J Intern Med. 2005; 257(1):6–17. [PubMed: 15606372]

44. Mosekilde L. Primary hyperparathyroidism and the skeleton. Clin Endocrinol (Oxf). 200869(1):1–19. [PubMed: 18167138]

45. Stein EM, Dempster DW, Udesky J, Zhou H, Bilezikian JP, Shane E, Silverberg SJ. Vitamin D deficiency influences histomorphometric features of bone in primary hyperparathyroidism. Bone. 2011; 48(3):557–61. [PubMed: 20950725]

46. Armbrecht HJ, Boltz MA, Hodam TL. PTH increases renal 25(OH)D3-1alpha - hydroxylase (CYP1alpha) mRNA but not renal 1,25(OH)2D3 production in adult rats. Am J Physiol Renal Physiol. 2003; 284(5):F1032–6. [PubMed: 12676737]

47. Calvi LM, Adams GB, Weibrecht KW, Weber JM, Olson DP, Knight MC, Martin RP, Schipani E, Divieti P, Bringhurst FR, Milner LA, Kronenberg HM, Scadden DT. Osteoblastic cells regulate the haematopoietic stem cell niche. Nature. 2003; 425(6960):841–6. [PubMed: 14574413]

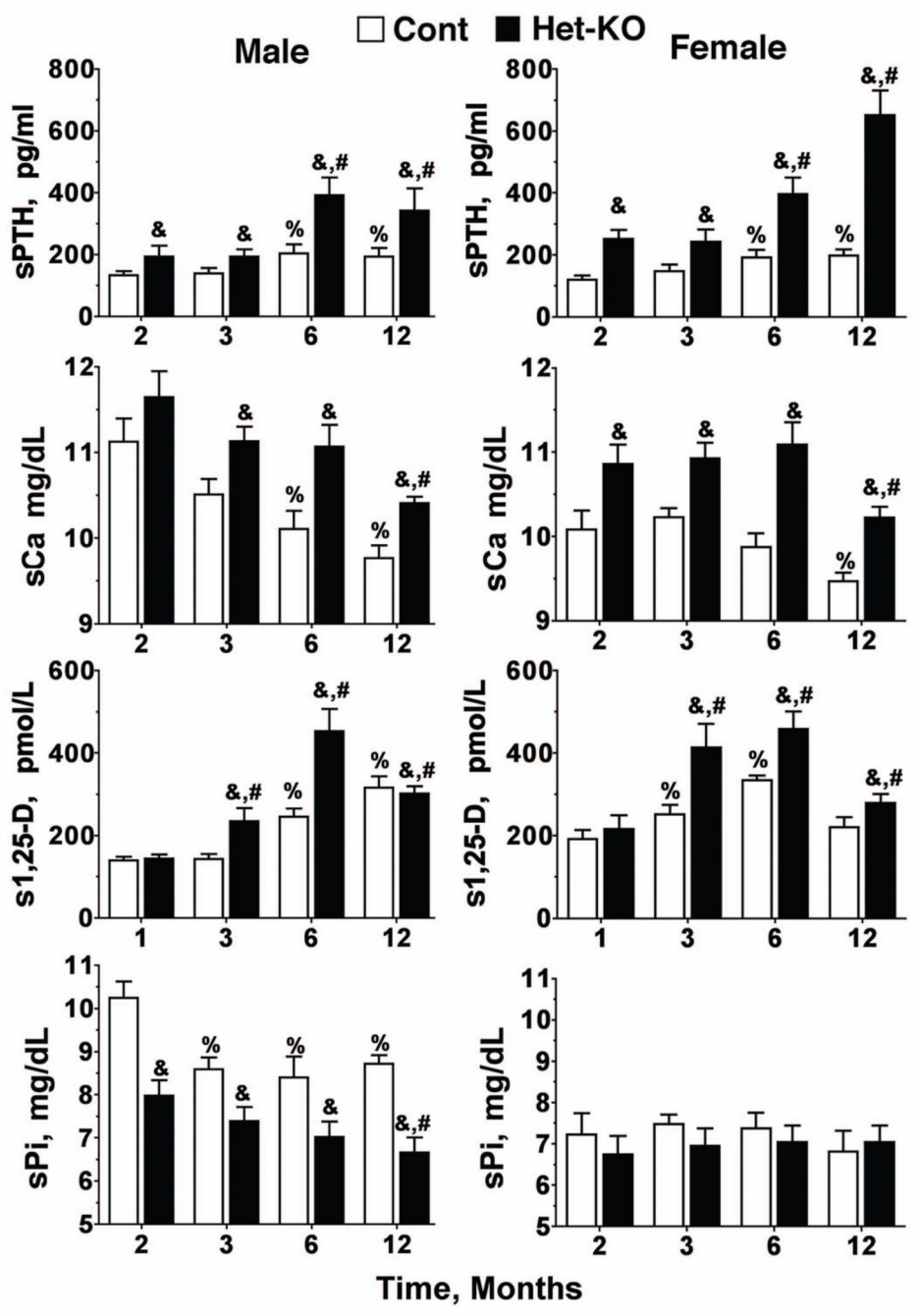

Figure 1. Age- and sex-dependent changes in serum minerals and calciotropic hormones in Control and Het-KO mice

Total calcium (sCa), phosphate (sPi), intact PTH (sPTH), and 1,25-dihydroxyvitamin D (s1,25-D) in sera from control (Cont, □) and heterozygous parathyroid-specific CaSR-KO (Het-KO, n) mice at 1, 2, 3, 6, and/or 12 months of age were determined as described in the Materials and Methods section. %: $p<0.05$ compared to Cont at 1 or 2 months of age; #: $p<0.05$ compared to Het-KO at 1 or 2 months of age; &: $p<0.05$ compared to Cont at the same age

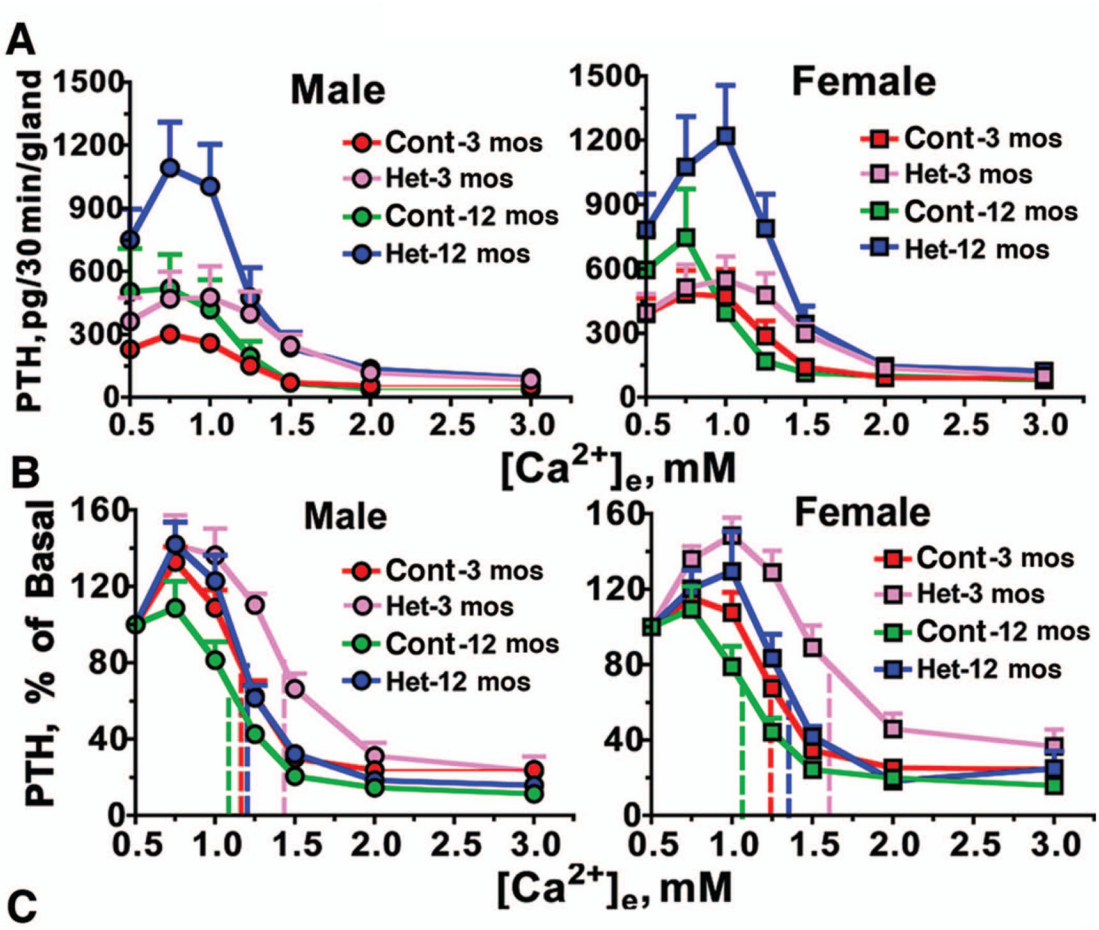

PTH Secretion Rate (pg/30min/gland)	Male				Female			
	3 months		12 months		3 months		12 months	
	Cont	Het	Cont	Het	Cont	Het	Cont	Het
^{PTH}R-max	309 ±28	498[a] ±110	588[a] ±158	1197[a,b,c] ±320	518 ±119	553 ±107	733[a] ±181	1282[a,b,c] ±279
^{PTH}R-min	49 ±5	82[a] ±12	31[c] ±6	80[b] ±12	84 ±15	98 ±9	59[c] ±11	80[b] ±12
Ca^{2+} set-point (mM)	1.19 ± 0.03	1.39[a] ± 0.02	1.07[a,c] ± 0.03	1.22[b,c] ± 0.04	1.24 ± 0.02	1.53[a] ± 0.04	1.04[a,c] ± 0.04	1.30[b,c] ± 0.03
a: p<0.05 vs 3 month Cont; b: p<0.05 vs 12 month Cont; c: p<0.05 vs 12 month Het								

Figure 2. Age- and sex-dependent changes in secretory capacity and Ca^{2+} set-point in Control and Het-KO PTGs

(**A**) Responses of PTH release at different $[Ca^{2+}]_e$ (pg/30 min/gland) in PTGs isolated from 3- and 12-month (mo) old male and female Cont and CaSR Het-KO (Het) mice were determined as described in the Materials and Methods. (**B**) Ca^{2+} dose-response curves shown in (A) were normalized and expressed as % of the PTH release at 0.5 mM Ca^{2+}. Dashed lines depict the Ca^{2+} set-points, defined as the $[Ca^{2+}]_e$ required to inhibit 50% of the maximal PTH release, and are tabulated along with their statistical significance in panel (**C**).

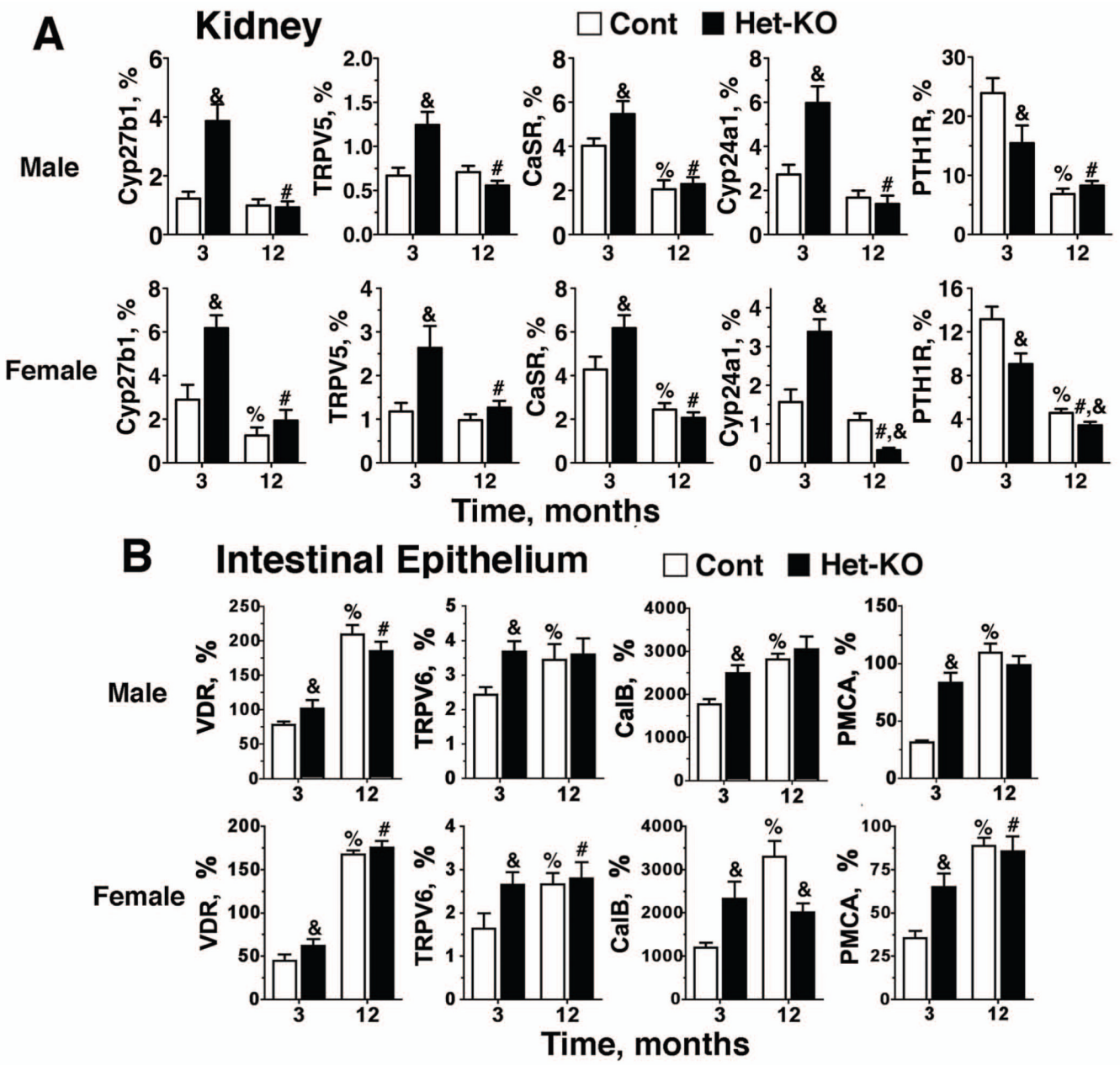

Figure 3. mRNA expression in the kidneys and intestinal epithelium in control and CaSR Het-KO mice

RNA was extracted from kidney (**A**) and intestinal epithelium (**B**) of 3- and 12-month-old male and female Het-KO and Control mice and analyzed by qPCR for the expression of Cyp27b1, TRPV5, CaSR, PTH1R, VDR, TRPV6, calbindin (CalB), or plasma membrane Ca^{2+}-ATPase (PMCA) using specific sets of TaqMan primers and probes as described in the Materials and Methods. RNA levels were normalized and expressed as % of expression of the ribosomal protein L-19. %, $p<0.05$ vs Control at 3 months of age; #, $p<0.05$ vs Het-KO at 3 months of age; &, $p<0.05$ vs Control of the same age.

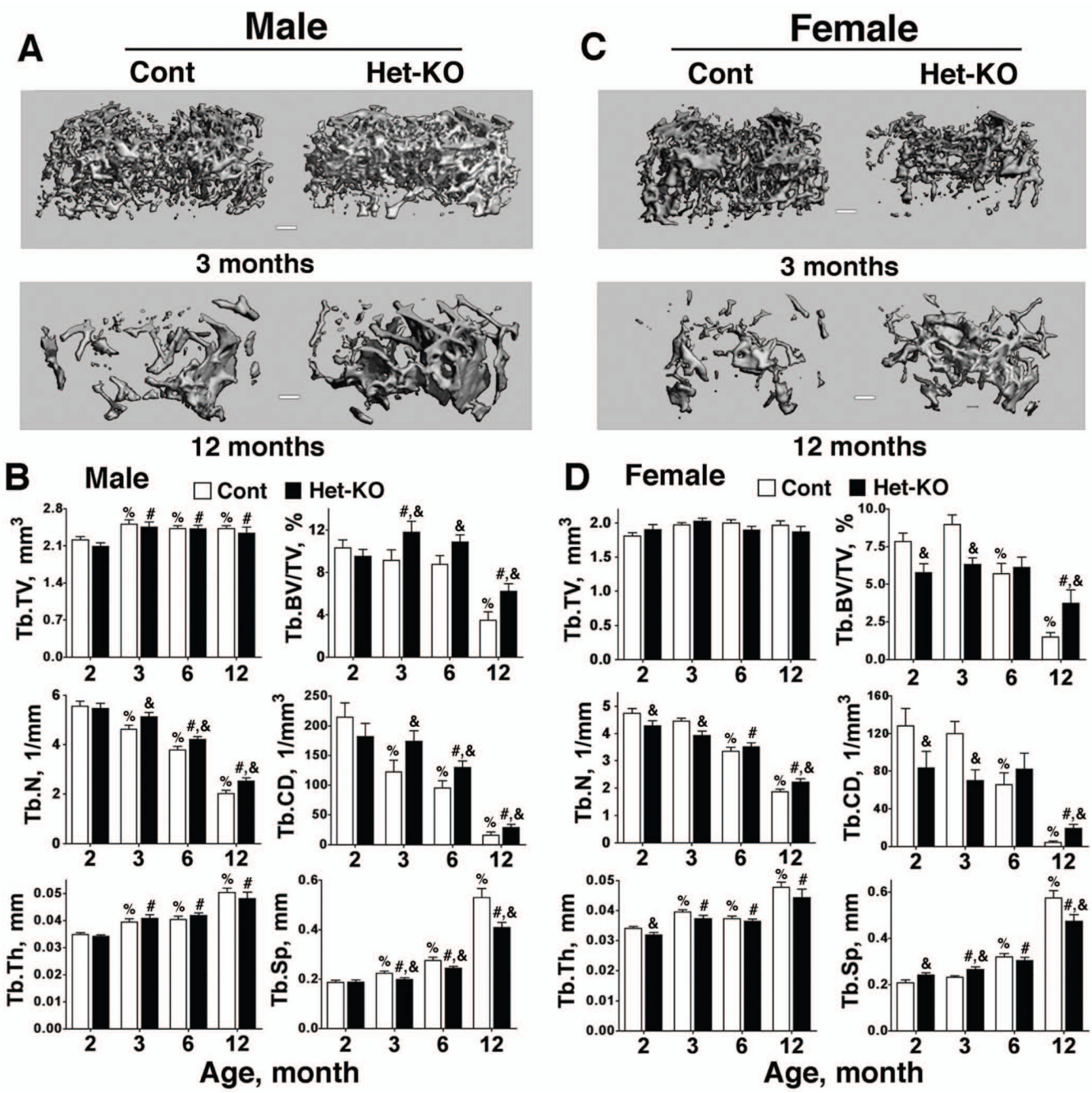

Figure 4. Trabecular (Tb) bone parameters in Control and Het-KO mice

Bone mass and structural parameters of Tb bone in distal femurs of male and female Control and Het-KO mice were assessed by ex vivo μCT as described in the Materials and Methods at 2, 3, 6, and 12 months of age. Representative 3D-reconstructed μCT images of Tb bones in male (**A**) and female (**C**) Control and Het-KO mice at 3 and 12 months of age. Quantifications of Tb bone parameters in male (**B**) and female (**D**) Cont (■) and Het-KO (□) mice. %, $p<0.05$ vs Cont at 2 months of age; #, $p<0.05$ vs Het-KO at 2 months of age; &, $p<0.05$ vs Cont of the same age.

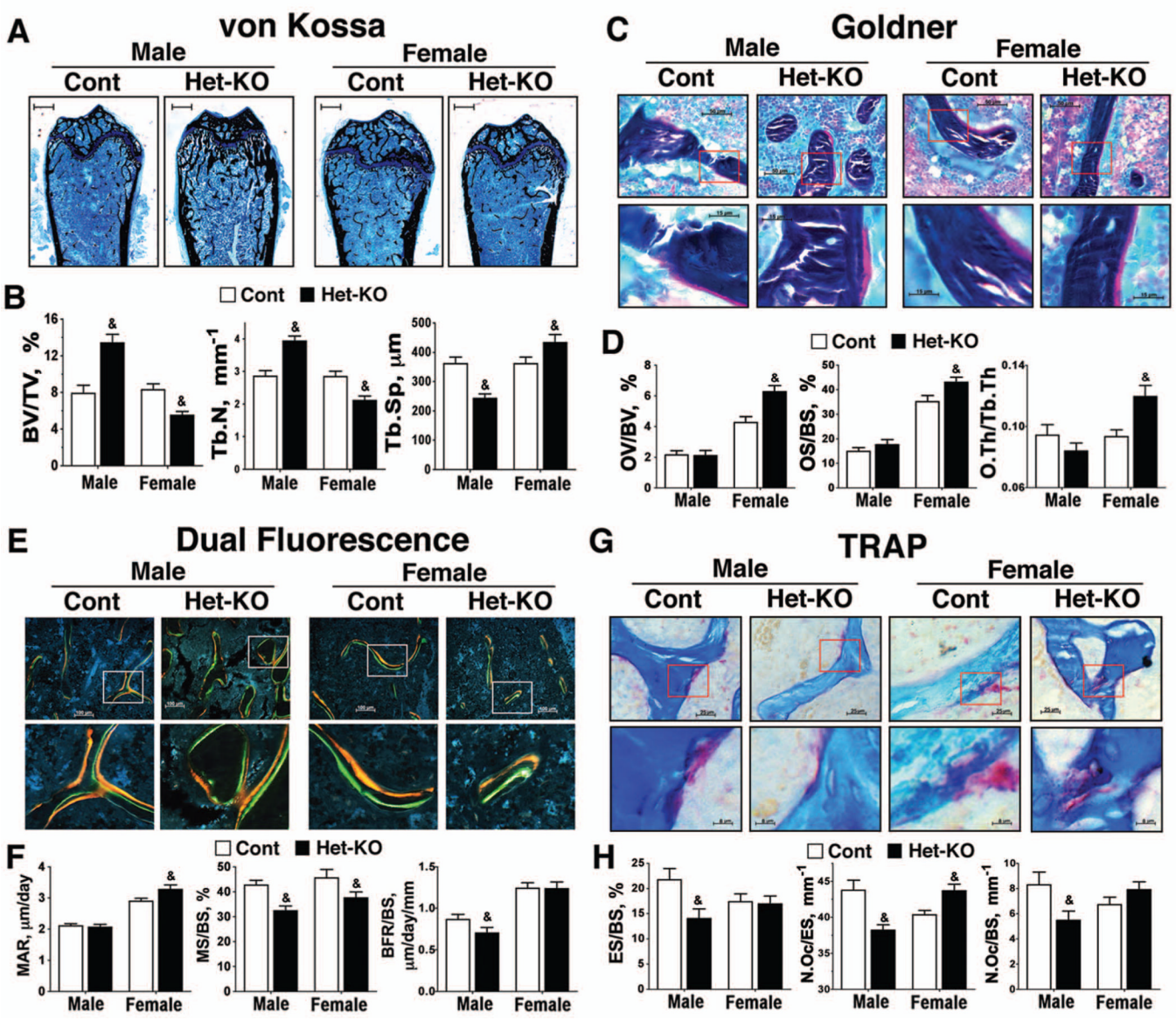

Figure 5. Bone histomorphometric analyses of Tb bone in Control and Het-KO mice

Bone mass and static and dynamic structural parameters of Tb bone in distal femur of male and female Control and Het-KO mice at 3 months of age were assessed by histomorphometry as described in the Materials and Methods with von Kossa and Tetrachrome (**A,B**), Goldner (**C,D**), and TRAP staining (**E,F**), and dual fluorescent calcein (green) and demeclocycline (orange) labeling (**G,H**). (**A,C,E,G**) Representative histological images for each staining with low (top panels) and high (bottom panels) power views. Red and white boxes indicate the regions enlarged and shown below. (**B,D,F,H**) Quantifications of static and dynamic bone parameters in male and female Cont (■) and Het-KO (□) mice.

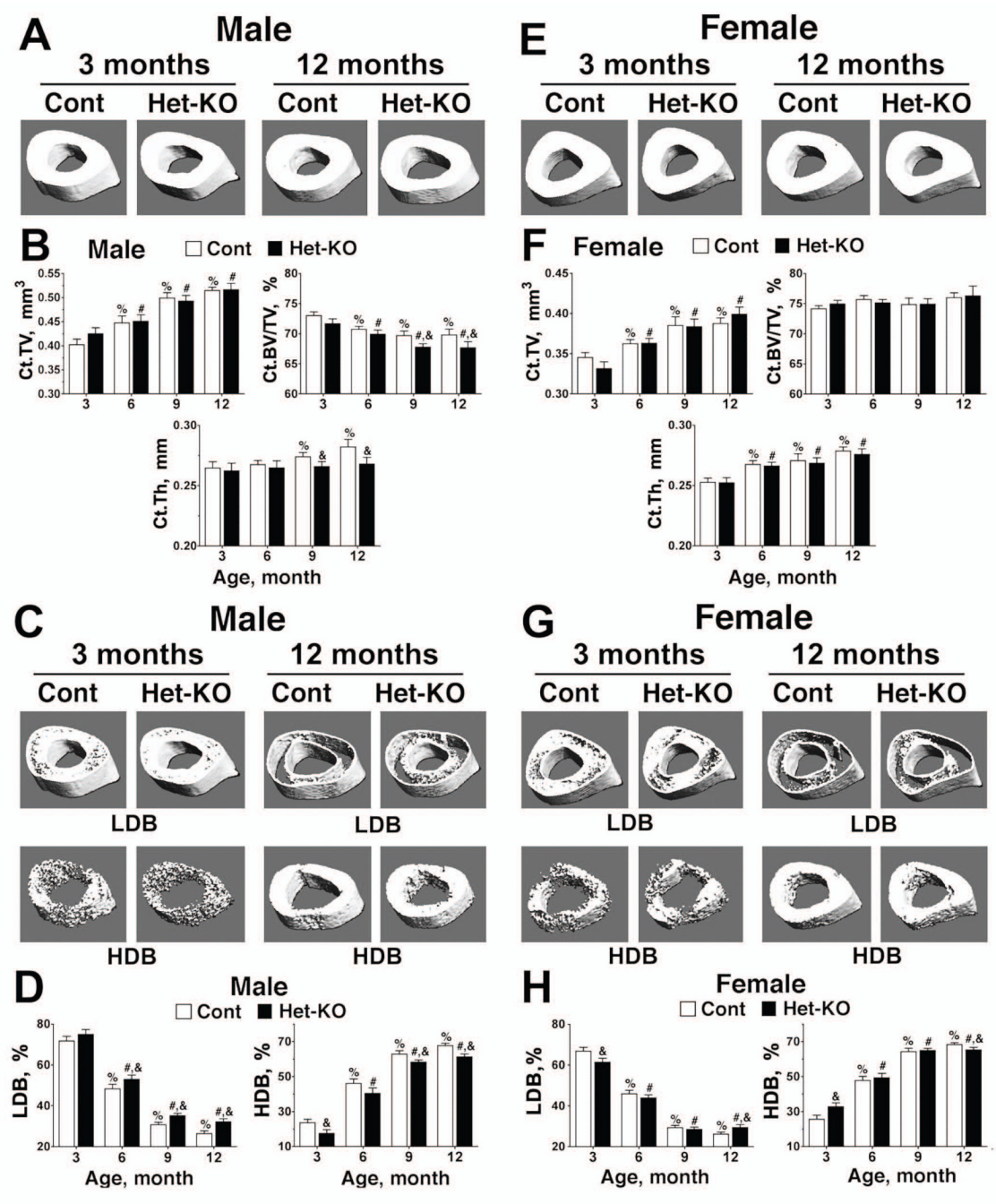

Figure 6. Age- and sex-specific responses of cortical (Ct) bone to chronic HPT

Bone mass and structural parameters of Ct bone at the tibulo-fibular junction (TFJ) of Cont and Het-KO mice were assessed by ex vivo μCT as described in the Materials and Methods at 3, 6, 9, and 12 months of age. (**A,C,E,G**) Representative 3D-reconstructed μCT images of Ct bones in male and female Cont and Het-KO mice at 3 and 12 months of age. (**B,F**) Quantifications of structural parameters for overall Ct bone, which contains >420 mg HA/mm^3, in male (**B**) and female (**F**) Cont (n) and Het-KO (□) mice. (**D,H**) Quantifications of low density bone (LDB), which contains 420-1400 mg HA/mm^3, and high density bone (HDB), which contains >1400 mg HA/mm^3, fractions in male (**D**) and female (**H**) Cont (n)

and Het-KO (□) mice. %, $p<0.05$ vs Cont at 3 months of age; #, $p<0.05$ vs Het-KO at 3 months of age; &, $p<0.05$ vs Cont of the same age.